Influence of winter and summer surface wind anomalies on Summer Arctic sea ice extent

Masayo Ogi [1], Koji Yamazaki [2] and John M. Wallace [3]

[1] Japan Agency for Marine-Earth Science and Technology, Yokohama, Japan (masayo.ogi@jamstec.go.jp)

[2] Faculty of Environmental Earth Science, Hokkaido University, Sapporo, Japan

[3] Department of Atmospheric Sciences, University of Washington, Seattle, Washington

Abstract

Based on a statistical analysis incorporating 925-hPa wind fields from the NCEP/NCAR Reanalyses, it is shown that the combined effect of winter and summer wind forcing accounts for 50% of the variance of the change in September Arctic sea ice extent from one year to the next (ΔSIE) and it also explains roughly 1/3 of the downward linear trend of SIE over the past 31 years. In both seasons meridional wind anomalies to the north and east of Greenland are correlated with September SIE, presumably because they modulate the export of ice through Fram Strait. Anticyclonic wind anomalies over the Beaufort Sea during summer favor low September SIE and have contributed to the record-low values in recent summers, perhaps by enhancing the flux of ice toward Fram Strait in the trans-polar drift.

1. Introduction

The dramatic retreat of Arctic sea ice extent (SIE) during recent decades, especially during summer [*Serreze et al*., 2007; *Comiso et al.*, 2008] has been attributed to changing patterns of surface winds [*Rigor et al.*, 2002; *Rigor and Wallace* 2004], ocean currents [*Polyakov et al.*, 2005; *Shimada et al.*, 2006], and downward energy fluxes from the atmosphere [*Francis and Hunter*, 2007; *Perovich et al*., 2007].

In September 2007, Arctic SIE reached its lowest value since microwave satellite measurements began in 1979. Most climate models have underestimated the observed decline of Arctic SIE: the observed 2007 minimum was much lower than simulated in any of the models participating in the Intergovernmental Panel on Climate Change Fourth Assessment Report (IPCC AR4) [*Stroeve et al*, 2007; *Boe et al.* 2009]. The causes of the rapid decline in SIE remain uncertain.

Several recent studies have investigated the variations of Arctic SIE that occur in association with the dominant patterns of atmospheric circulation variability. *Rigor et al.* [2002] suggested that the positive polarity of the wintertime Arctic Oscillation (AO) induces negative anomalies in sea ice during the following summer. *L'Heureux et al*., [2008] suggested that the summertime Pacific-North American (PNA) pattern has played a role in the rapid decline in summer SIE. The so-called "winter dipole anomaly", which corresponds to the second EOF of the sea level pressure (SLP) field

over the polar cap region, has been linked to the export of Arctic sea ice [*Wu et al.*, 2006]. EOF-3 of the Northern Hemisphere SLP field has also been mentioned in connection with the recent sea ice decline [*Overland and Wang*, 2005]. *Ogi and Wallace* [2007] have shown that years of low September SIE tend to be characterized by anticyclonic summertime circulation anomalies over the Arctic Ocean. The extreme loss of sea ice during summer 2007 was accompanied by strong anomalous anticyclonic flow, with Ekman drift out of the marginal seas toward the central Arctic [*Ogi et al.*, 2008]. Hence, there is evidence that both winter and summer atmospheric circulation anomalies influence the extent of Arctic sea ice at the end of the summer season.

In this study, we consider how the winds force changes in September Arctic SIE from one year to the next and how they might have contributed to the observed multidecadal decline in ice extent. In contrast to most previous studies, we make use of wind fields rather than pressure fields and the domain in our study extends beyond the Arctic Ocean to encompass the region of ice export through Fram Strait and southward along the east coast of Greenland.

2. Data and methods

September SIE data from 1979 to 2009 are based on *Comiso and Nishio* [2008].

To represent the wind field, we use the National Centers for Environmental Prediction/National Center for Atmospheric Research (NCEP/NCAR) reanalysis dataset from 1979 to 2009 [*Kistler et al.,* 2001]. First, the 925-hPa wind fields are regressed on September SIE to determine the seasonally-varying wind pattern that is linearly related to the subsequent September SIE. The resulting regression maps are shown in the paper and the corresponding correlation maps (not shown) are used as indicated below. Here, "winter" is defined as JFMAM mean (the average for January through May). Similarly, "summer" is defined as JJAS (the average for June through September).

Wind indices for each season in each calendar year are obtained by projecting the JFMAM and JJAS wind anomaly fields for each year onto the corresponding correlation patterns. We then use the standardized time series of these winter and summer wind indices as predictors in a linear model to predict difference in September SIE from one year to the next (ΔSIE).

3. Results

Figure 1 shows the patterns of the winter and summer 925-hPa wind anomalies regressed upon inverted one-year difference September SIE (-ΔSIE) time series (Figs. 1a and 1b) and the inverted detrended September SIE time series (Figs. 1c and 1d) for

the period of record 1979-2009. Winter and summer linear trends as determined from a least squares best fit regression are shown for comparison in Figs.1e and 1f.

The 925-hPa wind anomalies in the winter preceding a negative ΔSIE year or a low September SIE year exhibit a strong northerly component to the north and east of Greenland in both for the one-year difference ($-\Delta$SIE) data (Fig. 1a) and the detrended data (Fig. 1c). This pattern is suggestive of an enhanced rate of flow of sea ice along the climatological-mean wintertime ice edge from the Barents and Kara Seas and out through Fram Strait. Such a transport would act to reduce the areal coverage of Arctic sea ice. Although the winter trend pattern over the Arctic Ocean (Fig. 1e) is by no means identical to the regression patterns (Figs. 1a and 1c), the features over the Barents Sea, Fram Strait and the subpolar North Atlantic are remarkably similar; i.e., they are also suggestive of enhanced forcing of sea ice transport toward and out through Fram Strait.

The patterns of summer winds regressed on $-\Delta$SIE (Fig. 1b) and detrended September SIE (Fig. 1d) are both characterized by anticyclonic 925-hPa wind anomalies over the Arctic Ocean. The anticyclonic flow is directed from the Chukchi Sea across the Arctic Ocean toward Fram Strait, thus favoring enhanced sea ice export into the Atlantic, as in winter, but with the ice coming from a different direction. In summer, when the Arctic sea ice is thin and there are large expanses of open water, the sea ice

movement is close to free drift and hence the response of the sea ice to the wind forcing may be larger than in winter. In the summer pattern associated with the linear trend (Fig. 1f) the anticyclonic gyre is more restricted to the Beaufort Sea, but it is also characterized by flow from the Chukchi Sea across the Arctic Ocean toward Fram Strait. In all six panels of Fig. 1, the dominant feature in the wind field is the anomalous northerly flow over and around Fram Strait.

Now we assess the influence of the winter and summer atmospheric circulations on the changes in September Arctic SIE from one year to the next (ΔSIE), making use of regression analysis. We first generate winter and summer wind indices by projecting the 925-hPa wind anomalies for each calendar year onto the correlation patterns corresponding to the regression patterns shown in Fig. 1, weighting each grid point in the summation by the area that it represents; i.e., by the cosine of its latitude. The domain used in these projections is the oceanic region north of 65°N and is the same one used in our previous studies [*Ogi and Wallace*, 2007; *Ogi et al.* 2008].

Time-series of the winter and summer indices obtained in this manner, with reference to -ΔSIE, are shown in Fig. 2a. The indices show positive trends of 0.252 standard deviation per decade (winter) and 0.608/decade (summer) during the 30 year

period of record (1980-2009). The winter index increases occurred mainly during the first half of the record, while the increases in summer index occurred later in the record.

In 2007 when the record-low minimum in September SIE was observed, the summer index exhibited a record high positive value and the winter index a moderately high positive value. In contrast, in 1996 when the record-high maximum was observed, both winter and summer indices exhibited near-record low negative values.

Using the two wind indices shown in Fig. 2a, ΔSIE is predicted by a multiple regression model with cross validation, withholding one year at a time in making regression model and predicting ΔSIE for the withheld year. Results are shown in Figure 2b; the correlation coefficient is 0.71. The regression coefficients for winter and summer winds are –0.585 and –0.244, respectively. The prediction scheme based on the cross validated results is statistically significant at the 99.9% level and accounts for 50% of the variance of ΔSIE time series.

Having shown that winter and summer wind forcing influence September ΔSIE, we will now take into account the preconditioning of the sea by introducing into the regression model the data for September SIE for the previous year. Figure 2c shows the time series of observed and predicted current September SIE based on cross-validated data, using as linear predictors the winter and summer indices shown in

Fig. 2a together with the observed SIE for the previous September. The results prove to be a good prediction of September SIE (cross-validated R=0.91). The regression coefficients without cross validation for previous September SIE, the winter wind and the summer wind are 0.593, -0.510 and -0.325, respectively. Considering that September SIE for the previous year is one of the predictors, the fact that the prediction replicates the downward trend in September SIE is in no way remarkable and does not prove that the trends in the wind indices in Fig. 2a are responsible for it.

Ogi et al. [2008] used a summer SLP index as the sole indicator of atmospheric conditions and they used the areal coverage of multi-year ice in May to represent the preconditioning of the ice. The correlation coefficient of the predicted September SIE based on the previous September SIE, the winter wind and the summer wind indices shown in Fig. 2c has proven to be higher than that obtained by *Ogi et al.* [2008] (R = 0.91 versus R = 0.82). This result suggests that the wind anomalies in both the previous winter and the previous summer influence September SIE and that the flow of ice from Arctic Ocean toward Fram Strait, which was not specifically considered in our previous study, plays a key role. The higher correlation could also indicate that wind patterns are better predictors of September SIE than SLP patterns.

We repeat the above analysis using the correlation patterns and indices based on detrended data (Figs. 1c and 1d) in place of the one-year difference data. In this case only the winter and summer wind indices are used as predictors, but in deriving the indices we project the total wind anomalies, including trends, onto the correlation patterns. A similar methodology was used by *Thompson et al.* [2000]. The winter and summer indices show positive trends from 1979 to 2009 (0.339 and 0.387 per decade, respectively). Then, the September SIE is predicted using these two indices (Fig. 3b). The correlation coefficient with validation is 0.74, and the trends in observed and predicted September SIE are –0.779 and –0.266 per decade, respectively. Hence, it appears that about one-third of observed trend of September SIE is explained by the wind forcing alone.

4. Conclusions and discussion

We have shown results indicating that wind-induced, year-to-year differences in the rate of flow of ice toward and through Fram Strait play an important role in modulating September SIE on a year-to-year basis and that a trend toward an increased wind-induced rate of flow has contributed to the decline in the areal coverage of Arctic summer sea ice.

Kwok [2009] examined year-to-year variability and trends in ice outflow into the Greenland and Barents Seas for the period 1979-2007 on the basis of passive microwave brightness temperature and ice concentration and SLP data. He also found evidence of increased wind forcing of ice export through Fram Strait but in his analysis the increased rate of flow was accompanied by a trend toward decreased sea ice concentrations in this region, so that the actual export of ice through Fram Strait showed little, if any long term trend over the 29-year period of record. However, he reported a systematic increase in the flux of ice toward Fram Strait in the trans-polar drift, particularly during summer, consistent with the wind pattern in our Fig. 1f. Our results also serve to confirm recent findings of *Ogi and Wallace* [2007] and *Ogi et al*. [2008] that anticyclonic circulation anomalies over the Arctic during summertime favor low SIE and that the winds over the Arctic Ocean have exhibited a trend in this sense, especially during the past decade.

It is notable that the wind and patterns obtained in this study and the SLP patterns implied by them do not correspond to the teleconnection patterns emphasized in previous studies— i.e., the AO [*Rigor et al*., 2002], the PNA pattern [*L'Heureux et al*, 2008] and the Dipole Anomaly pattern [*Wu et al.*, 2006] — quite possibly because the methodology used in our study is different. In the studies cited above the dominant

spatial pattern of atmospheric variability pattern was obtained by EOF analysis and the expansion coefficient (or principal component) time series of that pattern was correlated with the time series of SIE. In contrast, the patterns identified in this study are obtained by direct linear regression of the 925 hPa wind field on time series of SIE. These regression patterns have significant projections onto the EOFs of the SLP field (e.g., the summer pattern resembles the summer Northern Hemisphere annular mode described by *Ogi et al*., 2004 to some extent). They are also similar to the SLP anomalies that drive anomalous sea ice motion across Fram Strait shown by Tsukernik et al. [2009]. But, the correspondence is not perfect.

We repeated the analysis keeping everything the same, but using the SLP field instead of 925-hPa wind field. The SLP patterns (not shown) are consistent with the 925 hPa wind patterns in Fig. 1 and time-varying indices derived from them (not shown) are very similar to those shown in Fig. 2a. However, it is notable that the correlations between the predicted and observed time series of September SIE are higher for the predictors based on wind data: R= 0.71 for wind versus 0.64 for SLP for the predicted and observed time series in Fig. 2b, 0.91 versus 0.85 for those in Fig. 2c, and 0.74 versus 0.49 for those shown in Fig. 3b. The statistical correlations between SIE and wind are higher than those between SIE and SLP because the physical relationship is

more direct.

The diagnostics used in this study may be useful for describing and comparing how the sea ice fields in climate models respond to the variations in the wind field. It would also be of interest to make a more direct comparison between the wind fields examined in this study and the two-dimensional field of satellite-derived ice-area flux examined in the study of *Kwok* [2009].

Acknowledgments

We thank I. Rigor for providing the September SIE data. We would like to thank J. Walsh and C. Deser for helpful comments and suggestions. J.M. Wallace was supported by the Climate Dynamics Program of the U.S. National Science Foundation under Grant GA 0812802

References

Boe J., A. Hall, and X. Qu (2009), September sea-ice cover in the Arctic Ocean projected to vanish by 2100. *Nature Geoscience,* doi:10.1038/NGEO467.

Comiso, J. C., and F. Nishio (2008), Trends in the sea ice cover using enhanced and compatible AMSR-E, SSM/I, and SMMR data. *J. Geophys. Res,* 113, C02S07,

doi:10.1029/2007JC004257.

Comiso, J. C., C. L. Parkinson, R. Gersten, and L. Stock (2008), Accelerated decline in the Arctic sea ice cover, *Geophys. Res. Lett.*, 35, L01703, doi:10.1029/2007GL031972.

Francis, J. A., and E. Hunter (2007), Drivers of declining sea ice in the Arctic winter: A tale of two seas, *Geophys. Res. Lett.*, 34, L17503, doi:10.1029/2007GL030995.

Kistler R, E. Kalnay, and co-authors (2001), The NCEP-NCAR 50-year reanalysis: Monthly means CD-ROM and documentation. Bull. Amer. Meteor. Soc., 82(2), 247-267.

Kwok, R. (2009), Outflow of Arctic ocean sea ice into the Greenland and Barents seas: 1979-2007, *J. Clim.*, 22, 2438-2457.

L'Heureux, M. L., A. Kumar, G. D. Bell, M. S. Halpert, and R. W. Higgins (2008), Role of the Pacific-North American (PNA) pattern in the 2007 Arctic sea ice decline, *Geophys. Res. Lett.*, 35, L20701, doi:10.1029/2008GL035205.

Ogi, M., K. Yamazaki, and Y. Tachibana (2004), The summertime annular mode in the northern hemisphere and its linkage to the winter mode, *J. Geophys. Res*, 109, D20114, doi:10.1029/2004JD004514.

Ogi, M., and J. M. Wallace (2007), Summer minimum Arctic sea ice extent and the

associated summer atmospheric circulation. *Geophys. Res. Lett.*, 34, L12705, doi:10.1029/2007GL029897.

Ogi, M., I. G. Rigor, M. G. McPhee, and J. M. Wallace (2008), Summer retreat of Arctic sea ice: Role of summer winds, *Geophys. Res. Lett.*, 35, L24701, doi:10.1029/2008GL035672.

Overland, J. E., and M. Wang (2005), The third Arctic climate pattern: 1930s and early 2000s, *Geophys. Res. Lett.*, 32, L23808, doi:10.1029/2005GL024254.

Perovich, D. K., B. Light, H. Eicken, K. F. Jones, K. Runciman, and S. V. Nghiem (2007), Increasing solar heating of the Arctic Ocean and adjacent seas, 1979-2005: Attribution and role in the ice-albedo feedback, *Geophys. Res. Lett*., 34, L19505, doi:10.1029/2007GL031480.

Polyakov, I. V. and 22 co-authors (2005), One more step toward a warmer Arctic, *Geophys. Res. Lett.*, 32, L17605, doi:101029/2005GL023740.

Rigor, I. G., J. M. Wallace, and R. L. Colony (2002), Response of sea ice to the Arctic Oscillation, *J. Clim.*, 15, 2648-2663.

Rigor, I. G. and J. M. Wallace (2004), Variations in the age of Arctic sea-ice and summer sea-ice extent, *Geophys. Res. Lett.*, 31, L09401, doi:10.1029/2004GL019492.

Serreze, M. C., M. M. Holland, and J. Stroeve (2007), Perspectives on the Arctic's

shrinking sea-ice cover, *Science*, 315, 1533-1536.

Shimada, K., T. Kamoshida, M. Itoh, S. Nishio, E. Carmack, F. McLaughlin, S. Zimmermann, and A. Proshutinsky (2006), Pacific Ocean inflow: Influence on catastrophic reduction of sea ice cover in the Arctic Ocean. *Geophys. Res. Lett.*, 33, L08605, doi:10.1029/2005GL025624.

Stroeve, J., M. M. Holland, W. Meier, T. Scambos, and M. Serreze (2007), Arctic sea ice decline: Faster than forecast. *Geophys. Res. Lett.*, 34, L09501, doi:10.1029/2007GL029703.

Thompson, D. W. J., J. M. Wallace, and G. C. Hegerl (2000), Annular modes in the extratropical circulation. Part Ⅱ. Trends, *J. Clim.*, 13, 1018-1036.

Tsukernik, M., C. Deser, M. Alexander, and R. Tomas (2009), Atmospheric forcing of Fram Strait sea ice export: a closer look. Clim. Dyn. doi:10.1007/s00382-009-0647-z.

Wu, B., J. Wang, and J. E. Walsh (2006), Dipole anomaly in the winter Arctic atmosphere and its association with sea ice motion, *J. Clim*., 19, 210-225.

Figure Captions

Figure 1: (a) Wind at 925 hPa in winter (JFMAM) regressed on the inverted one-year difference of September Arctic SIE (-ΔSIE) for the period 1979-2009. (b) As in Figure

1a, but in summer (JJAS) (c) Detrended wind at 925 hPa in winter regressed on the time series of inverted, detrended September SIE. (d) As in Figure 1c, but for summer. (e) The linear trend of 925-hPa winter wind (per decade) (f) As in Figure 1e, but for summer wind.

Figure 2: (a) Time-series of standardized winter (white) and summer (black) indices based on 925-hPa correlation patterns obtained by regressing JFMAM-mean wind fields for each year upon the one-year difference of September SIE from the previous year to the current year ($-\Delta$SIE). The corresponding regression patterns are shown in Figure 1a and 1b. (b) Observed (black circles) and predicted (open squares) one-year difference of September SIE (ΔSIE) using a prediction model with winter and summer wind indices in Fig. 2a as predictors, with cross validation (R=0.71) (c) Observed (black circles) and predicted (open squares) September SIE, including, as a third predictor, the previous September SIE (R=0.91).

Figure 3: (a) As in Figure 2a but using detrended 925-hPa wind patterns regressed on detrended September SIE, shown in Figure 1c and 1d. (b) Observed (black circles) and predicted (open squares) September SIE prediction model based on cross validated dataset using winter and summer indices shown Figure 3a (R=0.74).

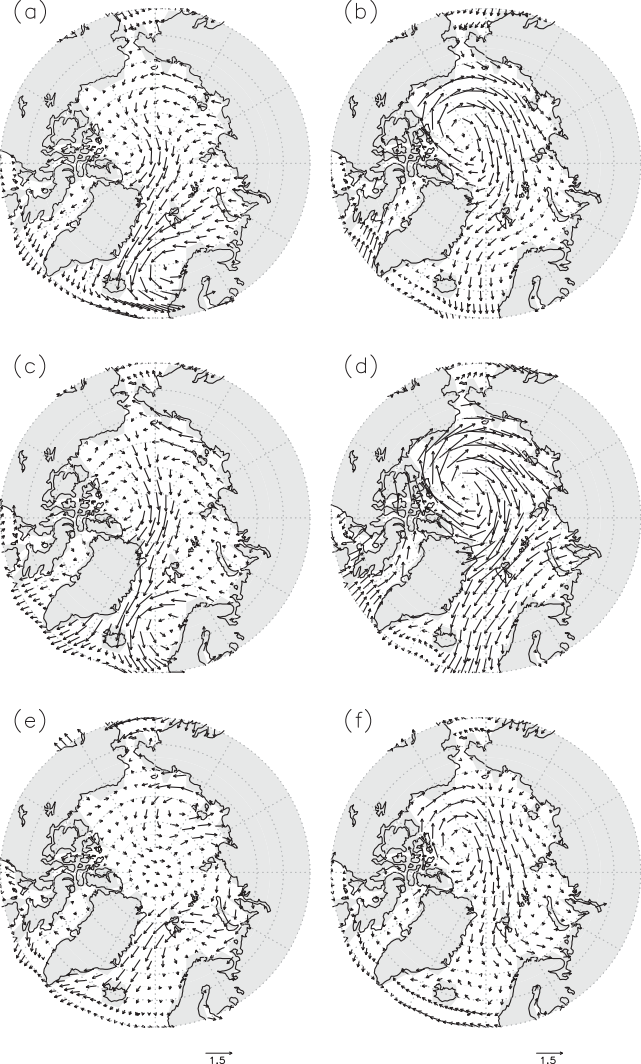
(a)
(b)
(c)
(d)
(e)
(f)
1.5
1.5

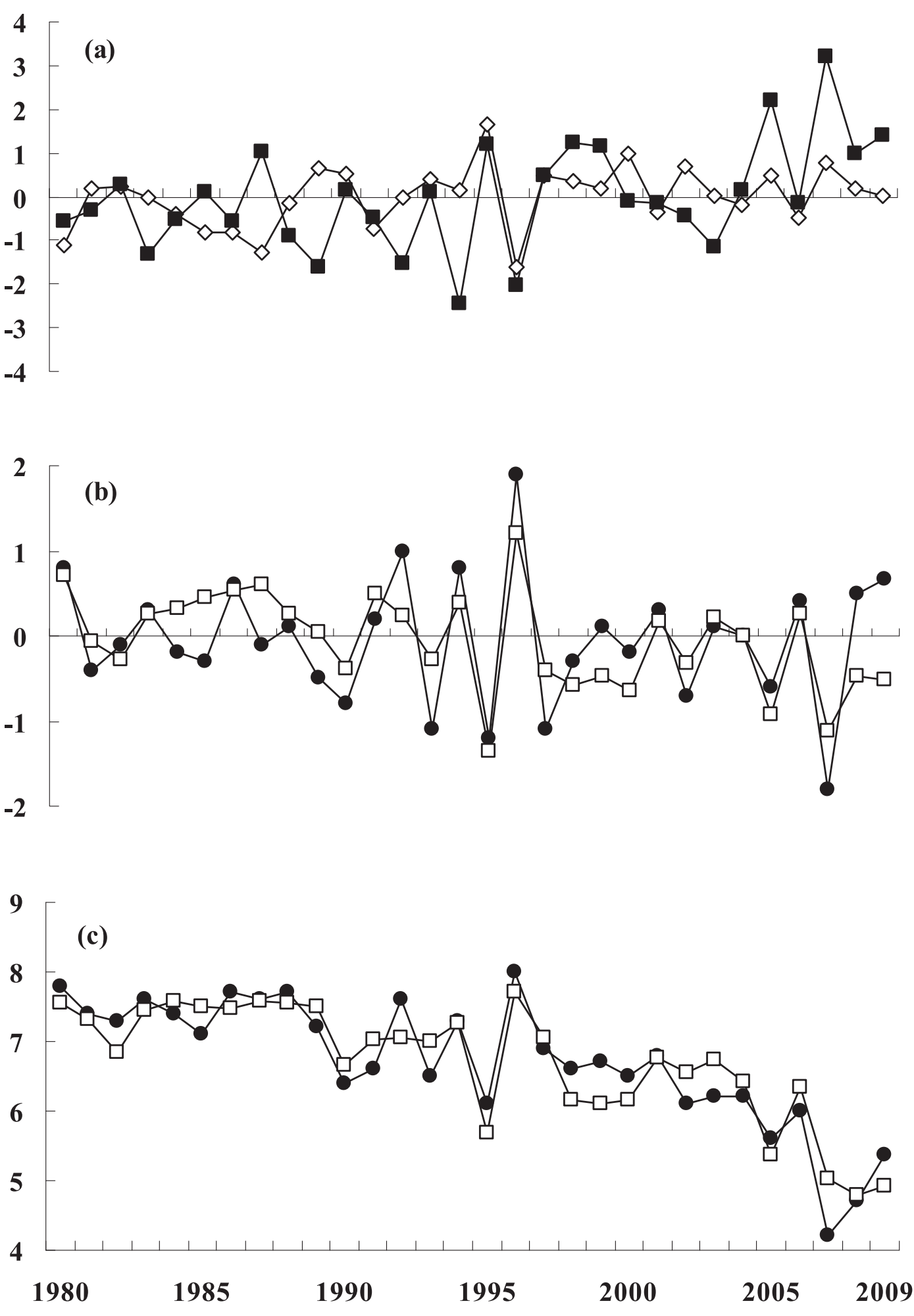
(a)
4
3
2
1
0
-1
-2
-3
-4
(b)
2
1
0
-1
-2
(c)
9
8
7
6
5
4
1980
1985
1990
1995
2000
2005
2009

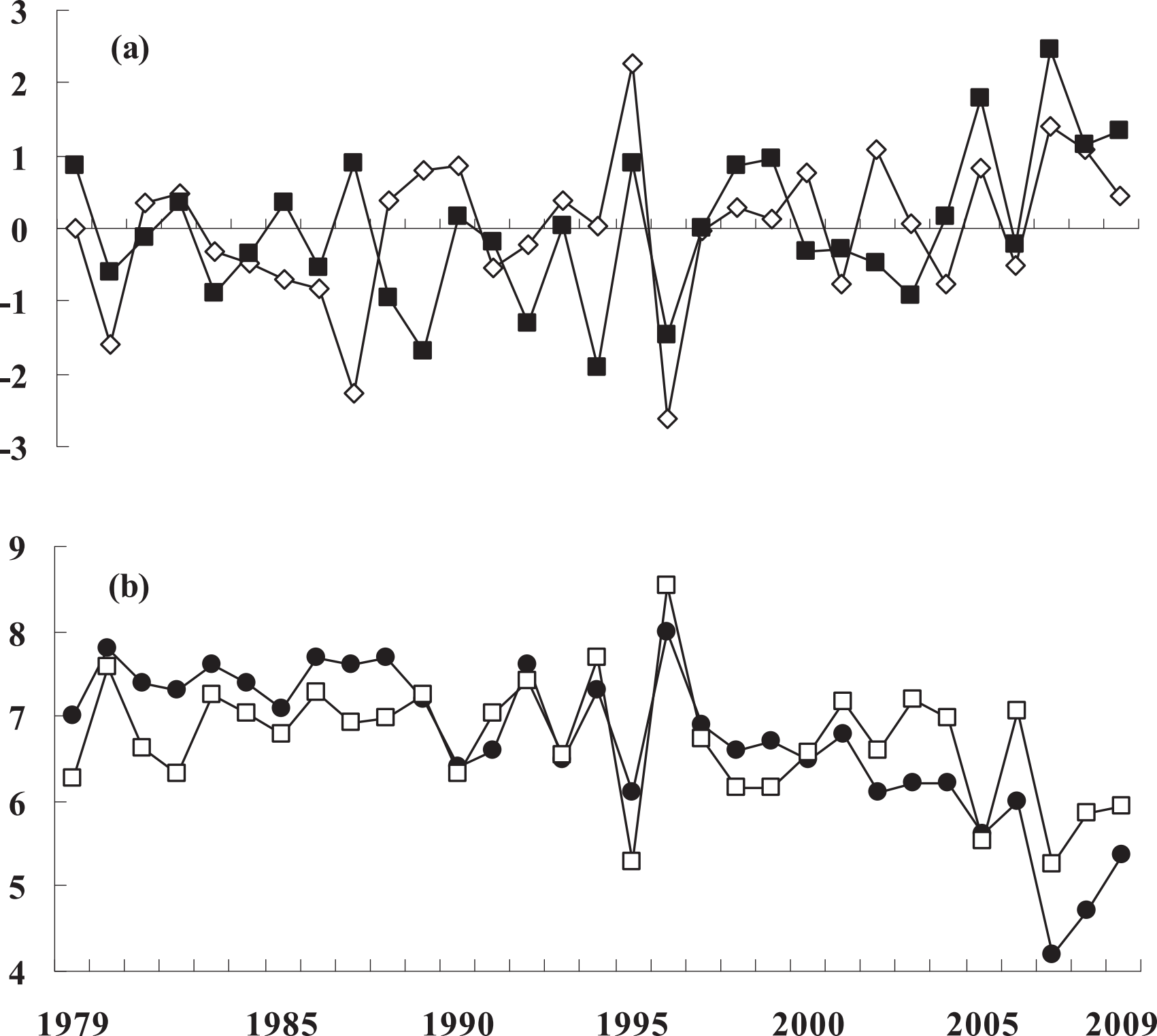
(a)
3
2
1
0
-1
-2
-3
(b)
9
8
7
6
5
4
1979
1985
1990
1995
2000
2005
2009